Journal of the Korean Society
for Marine Environmental Engineering
Vol.2, No.2, pp. 70~77, Aug. 1999

Behavior of Oil-Water Interface between Tandem Fences

by
Kwan Hyoung Kang[1] and Choung Mook Lee[2]

이중 유벽 사이의 기름과 물의 계면의 거동

강관형[1], 이정묵[2]

Abstract

The disturbance of oil-water interface confined between tandem fences caused by a sequence of traveling vortices below the interface is investigated. The traveling vortices are assumed to be those detached from the tip of the fore fence. The potential flow is assumed and the density interface is replaced as a sheet of vortex. The shape of the interface is predicted by tracing a finite number of marker particles placed at the interface. The velocity of the marker particles is determined by the Biot-Savart integral along the vortex sheet plus the contribution from the traveling point vortices. The rate of change of vortex-sheet strength is predicted by using an evolution equation for vorticity. The calculated results obtained for various conditions demonstrate that the large amplitude of interfacial wave following the moving vortex can be generated by the vortices.

요 약

와류에 의한 이중 유벽 사이에 가두어진 기름층과 물의 계면의 교란에 대하여 고찰하였다. 와류는 전부 유벽의 끝에서 발생되는 것으로 간주하였다. 유동장의 해석을 위하여 포텐셜 유동 가정하에 계면을 와 특이점 분포면(vortex sheet)으로 나타내었다. 계면의 형상은 계면에 유한개의 가상의 입자를 설정한 후 그 위치를 추적하여 구하였다. 입자의 속도는 와 분포면에 의해서 유발되는 속도를 Biot-Savart 적분을 통해 구하고 여기에 이동하는 점와류(point vortex)에서 유발되는 속도를 합하여 구하였다. 시간에 대한 와 분포면상의 와도의 변화는 계면에서의 와도 방정식을 해석하여 구하였다. 여러 조건하에서 계산된 결과를 바탕으로 상당한 파고의 계면파가 전부 유벽 하단에서 발생되는 와류에 의하여 생성될 수 있음을 입증하였다.

Keywords: oil fence (유벽), oil boom (오일붐), interfacial wave (계면파), two-layer flow (다층유동), vortex shedding (와 방출)

(1) 정회원, 첨단유체공학 연구센터
(2) 정회원, 삼성중공업, 조선플랜트 연구센타

1. Introduction

The use of an oil fence in a sea environment is limited due to the waves and currents. It has been suggested to place another fence in tandem so as to contain the contaminant at the shelter formed between the two fences (Delvigne [1987]). Lo [1996] has shown, through a model experiment, that the leaked oil beneath the fore fence can be recaptured if the distance between the two fences is greater than sixteen times the draft of the fore fence. Lee *et al.* [1998a] has reconfirmed the validity of the method, by applying the Lagrangian tracking method to simulate the trajectory of oil droplets leaked beneath the fore fence.

If the current speed exceeds a certain limit, the oil layer contained between the two oil fences can leak beneath the rear fence. The optimum distance between the two fences in which the leakage of oil can be minimized has been pursued by Lee *et al.*[1997], by measuring the leakage rate of kerosene oil contained between two model fences. It is shown that the containment capability is significantly dependent on the distance between the two fences, and that the optimum distance between the two fences is approximately eight times the draft of the fore fence.

When such a leakage takes place, it is observed that interfacial waves of relatively large amplitude are intermittently generated at the back of the fore fence. The waves travel towards the rear fence, collide and pile up at the face of the rear fence, and eventually leak when the piled volume exceeds the fence draft. Flow visualization of the water flow beneath the oil layer contained by tandem fences showed that a large-scale vortex moves with an interfacial wave. It is conjectured that the vortices detached from the edge of the fore fence excite the interface to develop such large amplitude interfacial waves. To find out if such a conjecture is valid, the behavior of a sequence of vortices in generating the interfacial wave in an infinite fluid domain is investigated.

A potential-flow method of vortex singularities is employed to simulate the process of wave generation at the interface of a two-density layer fluid by traveling vortices below the interface. The method has been successfully used in investigating the large amplitude surface waves (Longuet-Higgins and Cokelet [1976], Baker *et al.* [1982]). The method relies on representing the interface as a vortex sheet across which the normal velocity is continuous but the tangential velocity has a jump. Since the motion of the vortex sheet represents that of the interface, the shape of the interface can be predicted by tracing the motion of the marker particles placed on the vortex sheet. The velocity of the marker particle is given by the Biot-Savart integral of the vortex distribution together with the effect of the series of discrete vortices below the interface. To determine the rate of change of vortex strength, an evolution equation for the vortex strength which can be derived using the kinematic boundary conditions and the Bernoulli equation is invoked.

2. Method of Analysis

A two-dimensional motion of two superposed fluids of different densities ρ_1 and ρ_2 is considered. Hereafter, the index 1 refers to the lower fluid and 2 to the upper fluid, respectively. A right-handed Cartesian coordinate system, which is depicted in Fig. 1, is used. The origin is located at the undisturbed interface. The fluids interface is perturbed by vortices which are located at $(x_o \pm nL, y_o)$ along a line parallel to the horizontal x axis. The distance between the consecutive vortices is L and n is an integer. The vortices have a constant strength of Γ_o and moving with the uniform stream velocity u_o in the positive x direction. It follows then that the flow is periodic horizontally with the period of L.

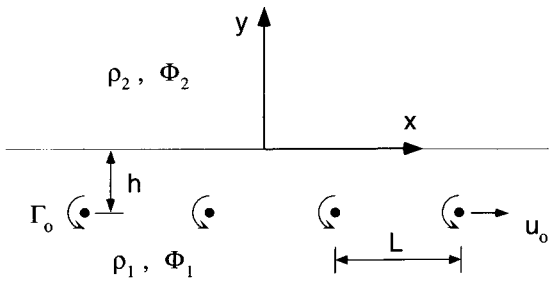

Fig. 1 Coordinate system

If a vortex sheet is placed at the interface, the complex velocity potential can be expressed by

$$\Phi(z,t) = \frac{1}{2\pi i}\int_{-\infty}^{\infty} \gamma'(s,t)\log[z-z'(s)]ds + \sum_{n=-\infty}^{\infty}\frac{\Gamma_o}{2\pi i}\log[z-z_o+nL],$$

where $z = x + iy$, $i = \sqrt{-1}$, $z'(s)$ represents a point on the sheet, $z_o(=x_o+iy_o)$ the position of a discrete point vortex, and γ' the vorticity which is positive if it is in the counter-clockwise direction.

A Lagrangian parameter e which represents the initial horizontal location of an imaginary marker particle placed at the fluids interface is introduced. Then, the above integral can be rewritten as

$$\begin{aligned}\Phi(z,t) &= \frac{1}{2\pi i}\int_{-\infty}^{\infty}\gamma(e,t)\log[z-z'(e)]de \\ &\quad + \sum_{n=-\infty}^{\infty}\frac{\Gamma_o}{2\pi i}\log[z-z_o+nL] \\ &= \frac{1}{2\pi i}\int_o^L \gamma(e,t)\log\sin\frac{\pi[z-z'(e)]}{L}de \\ &\quad + \frac{\Gamma_o}{2\pi i}\log\sin\frac{\pi[z-z_o]}{L}.\end{aligned} \tag{1}$$

In the above, γ is the vorticity in the Lagrangian coordinate, and is defined as $\gamma=\gamma' s_e$, in which $s_e = ds/de$. It should be noted that the interval of integration is reduced to a finite one by using the periodicity of the flow (Milne-Thomson [1968]).

Two complex velocity potentials Φ_1 and Φ_2 for each fluid are introduced. The complex velocity $q_j(=u_j+iv_j)$, where j = 1, 2, is related with the complex velocity potential as $q_j^* = d\Phi_j/dz$, in which the asterisk represents the complex conjugate. It is conventional to assume that the vortex sheet moves with the average velocity of fluid particle on both sides of the vortex sheet, i. e., $\tilde{q} = (q_1+q_2)/2$, where $\tilde{q}$ represents the velocity of the vortex sheet (Milne-Thomson [1968]). Then, the velocity of particles located on the vortex sheet can be obtained as

$$\begin{aligned}\frac{dZ^*(e,t)}{dt} &= \frac{d\Phi}{dz} \\ &= \frac{1}{2iL}\int_o^L \gamma(e',t-\Delta t)\cot\frac{\pi[Z(e,t-\Delta t)-z'(e')]}{L}de' \\ &\quad + \frac{\Gamma_o}{2iL}\cot\frac{\pi[Z(e,t-\Delta t)-z_o]}{L},\end{aligned} \tag{2}$$

where $Z = X(e,t) + iY(e,t)$ represents the position of the marker particles.

The above equation is the periodic form of the Birkhoff-Rott equation (Saffman [1992]). The evolution equation for vorticity $\gamma(e,t)$ is derived using the boundary conditions at the interface and the Bernoulli equations for the two fluids as follows (see Baker *et al.* [1982]):

$$\begin{aligned}\frac{d\gamma}{dt} &= -\frac{\sigma}{\rho}\frac{\partial\kappa}{\partial e} - 2A\left[\frac{du_s}{dt} - \frac{1}{2}\frac{\partial\tilde{q}^2}{\partial e}\right. \\ &\quad \left. + \frac{1}{8}\frac{\partial}{\partial e}\left(\frac{\gamma^2}{s_e^2}\right) + g\frac{\partial Y}{\partial e}\right],\end{aligned} \tag{3}$$

where $\tilde{u}_s = u\cdot t$, t the unit vector tangential to the interface, σ the interfacial-tension coefficient, g the gravitational acceleration, κ the curvature of the interface, $\tilde{q}^2 = \tilde{u}^2 + \tilde{v}^2$, $\bar{\rho} = (\rho_1+\rho_2)/2$, and $A = (\rho_1-\rho_2)/(\rho_2+\rho_1)$.

If the characteristic length, velocity, and time are chosen as L, Γ_o/L, and L^2/Γ_o, respectively, the primitive variables can be non-dimensionalized as follows:

$\bar{t} = t\Gamma_o/L^2$, $\bar{X} = X/L$, $\bar{Y} = Y/L$, $\bar{e} = e/L$, $\bar{u} = uL/\Gamma_o$, $\bar{x} = xL$, $\bar{\gamma} = \gamma/\Gamma_o$

The expressions of the Birkhoff-Rott equation (Eq. (2)), and the vorticity equation (Eq. (3)) with the above non-dimensional variables become

$$\frac{d\bar{Z}^*(\bar{e},\bar{t})}{d\bar{t}} = \frac{1}{2i}\int_o^1 \bar{\gamma}(\bar{e}')\cot\pi[\bar{Z}-\bar{z}'(\bar{e}')]d\bar{e}' + \frac{1}{2i}\cot\pi(\bar{Z}-\bar{z}_o), \quad (4)$$

$$\frac{d\bar{\gamma}}{d\bar{t}} = \frac{1}{W}\frac{\partial\bar{x}}{\partial\bar{e}} - \frac{1}{F^2}\frac{\partial\bar{Y}}{\partial\bar{e}} - 2A\left[\frac{d\bar{\tilde{u}}_s}{d\bar{t}} - \frac{1}{2}\frac{\partial\bar{\tilde{q}}^2}{\partial\bar{e}} + \frac{1}{8}\frac{\partial\bar{\gamma}^2}{\partial\bar{e}}\left(\frac{\bar{\gamma}^2}{s_e^2}\right)\right]. \quad (5)$$

Here bar indicates the non-dimensional variable. The Froude number ($F = \Gamma_o/\sqrt{L^3\tilde{g}}$) and the Weber number ($W = \bar{\rho}\Gamma_o^2/(\sigma L)$), in which $\tilde{g} = 2gA$, represent the strength of the pressure force generated by the vortices to the gravity force and to the surface tension, respectively.

Equations (4) and (5) are solved numerically. The detailed procedure of the numerical analysis is described in Lee *et al.* [1998b]. Here, a linear analysis for the evolution of the vortex sheet is performed using the Taylor series in time t, in order to examine the interface deformation in the initial stage, and to verify the numerical results. It is assumed that the interface $\bar{Z}(\bar{e},\bar{t})$ and vorticity can be expanded for a sufficiently small time t as

$$\bar{Z}^* = \bar{e} + \sum_{n=1}^{\infty}\bar{t}^n Z_n^*(\bar{e}), \quad (6a)$$

$$\bar{\gamma}(\bar{e},\bar{t}) = \sum_{n=1}^{\infty}\bar{t}^n G_n(\bar{e}). \quad (6b)$$

Initially, the interface is flat, and $\bar{\gamma}(\bar{e},\bar{t})$ is identically zero so that the non-dimensional Birkhoff-Rott equation is reduced to, for a sufficiently small time,

$$\left.\frac{d\bar{Z}^*(\bar{e},\bar{t})}{dt}\right|_{t=o} \simeq \frac{1}{2i}\cot\pi(\bar{e}-\bar{z}_o) \quad (7)$$

By substituting Eq. (6a) into Eq. (7), one obtains the following first order solution:

$$Z_1^*(\bar{e}) = \frac{1}{2i}\cot\pi(\bar{e}-\bar{z}_o). \quad (8)$$

Resolving the above equation into real and imaginary parts, one obtains

$$\bar{X}(\bar{e},\bar{t}) = \bar{e} + \frac{\bar{t}}{2}\frac{\sinh 2\pi\bar{y}_o}{\cosh 2\pi\bar{y}_o + \cos 2\pi(\bar{e}-\bar{x}_o)} \quad (9a)$$

$$\bar{Y}(\bar{e},\bar{t}) = -\frac{\bar{t}}{2}\frac{\sin 2\pi(\bar{e}-\bar{x}_o)}{\cosh 2\pi\bar{y}_o + \cos 2\pi(\bar{e}-\bar{x}_o)} \quad (9b)$$

From Eq. (5), the rate of change of vorticity can be approximated, for a small Froude number, as

$$\frac{d\bar{\gamma}}{dt} \simeq -\frac{1}{F^2}\frac{\partial\bar{Y}}{\partial\bar{e}} \quad (10)$$

If Eqs. (6b) and (9b) are substituted into Eq. (10), it follows that

$$\gamma(\bar{e}) = \frac{\pi t^2}{2F^2}\frac{1+\cos 2\pi(\bar{e}-\bar{x}_o)\cosh 2\pi\bar{y}_o}{[\cosh 2\pi\bar{y}_o + \cos 2\pi(\bar{e}-\bar{x}_o)]^2} \quad (11)$$

3. Results and Discussions

In Fig. 2(a), the linear solution for interface shape, for the Froude number of 0.1, is compared with the numerical results. In Fig. 2, τ is defined as L^2/Γ_o. The point vortex is located at $\bar{x}_o = 0.5$ and $\bar{y}_o = -0.3$, and assumed that the position of the vortex is unchanged. As shown in Fig. 2(a), the analytic solution almost coincides with the numerical solution at the initial stage. The difference between the two results becomes greater as time increases. This may be because the non-

linearity becomes important as the deformation of the interface becomes greater. In Fig. 2(b), the dimensionless vorticity which is obtained analytically is compared with the numerical solution. Like the shape of the interface, the two results agree fairly well at least for the initial stage.

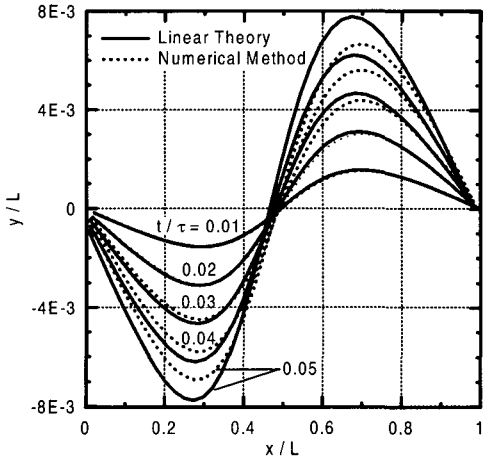

(a) interface shape

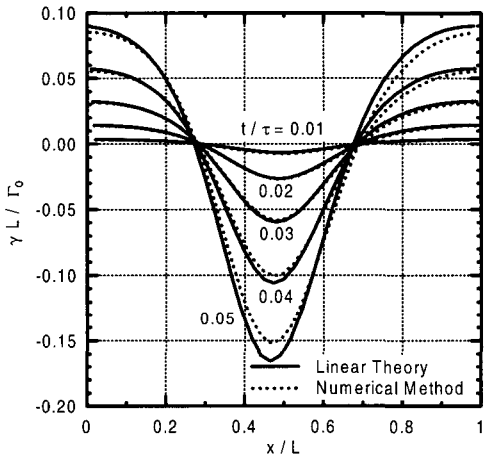

(b) vorticity

Fig. 2 Comparison between linear theory and numerical method for F=0.1, and ρ_2 / ρ_1=0.8

In the linear theory, the contribution of the vortex sheet, i. e., the integral term in Eq. (4) on the evolution of interface is not included. As long as the nonlinear effect is negligible, the vorticity will have a similar distribution to those shown in Fig. 2(b). This vorticity distribution on the vortex sheet can be approximated by three lumped point vortices which induce the flow pattern as described in Fig. 3(a). It is evident that the flow generated by the induced vorticity on the vortex sheet reduces the growth rate of the interfacial disturbances (see Fig. 3(b)). The result of the linear theory, therefore, over-estimates the peak values of interface location, as shown in Fig. 2(a).

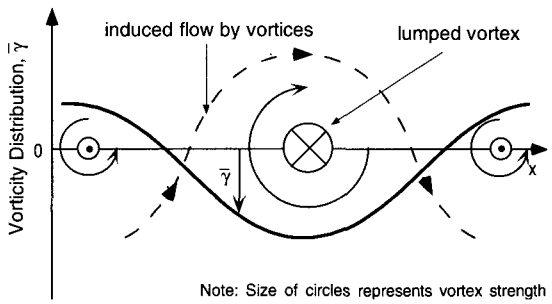

(a) flow induced by vortex sheet

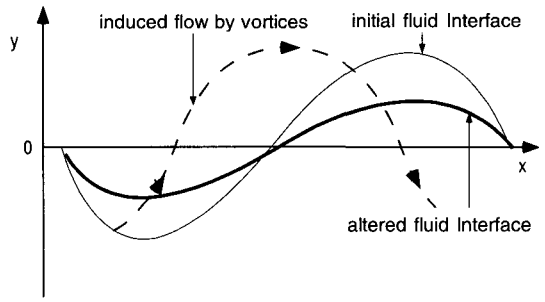

(b) effect of induced flow

Fig. 3 Effect of vortex sheet on interfacial shape

In Fig. 4 the temporal evolutions of the interface for two Froude numbers of 0.73 and 1.0 are shown. The other conditions are identical to the case of Fig. 2. At the initial stage, the shape of the interface is sinusoidal, which is consistent with the prediction of the linear theory (see Eq. (9)). As time increases, a large trough is formed at about $\bar{x}_o = 0.2$. When the Froude number is 1.0, the crest- to-trough

height of the trough becomes about 0.3L.

According to the numerical results, the trough continues to grow until a cusp is formed at the lowest point of the trough. In reality, the formation of a sharp cusp will be prevented by the interfacial breaking, viscous resistance, and interfacial tension. Thus, the current analysis method, which is based on the potential-flow assumption, may show a somewhat exaggerated cusp formation.

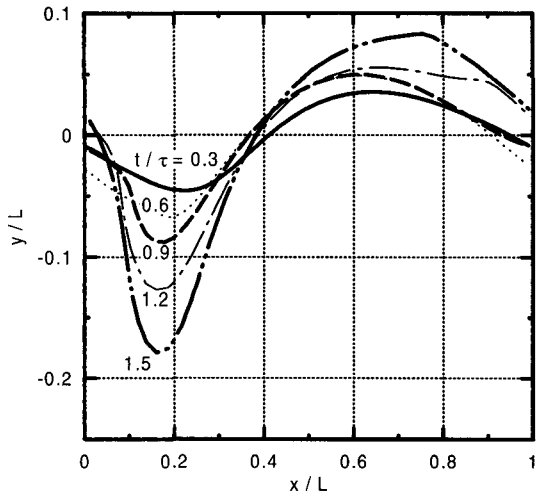

(a) F=0.73

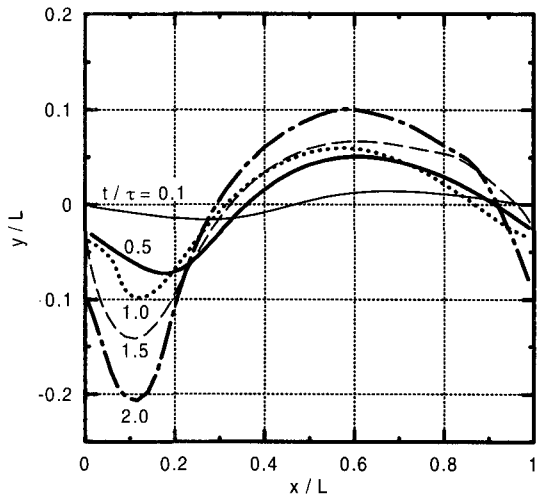

(b) F= 1.0

Fig. 4 Deformation of interface with time: ρ_2 / ρ_1 =0.8

In Fig. 5(a), the flow without the oil layer around the tandem fences are visualized for the separation distance of $10D$, where D is the draft of the fence. The vortical flow patterns are generated by isolated vortices. Under the same flow condition, kerosene oil was poured between the fences. Then, as shown in Fig. 5(b), periodic lumps were generated at the rear of the fore fence and traveled towards the rear fence. The leakage occurred when the traveling lumps dashed to the rear fence consecutively, which eventually pushed the oil column downward along the face of the rear fence to the tip of the fence.

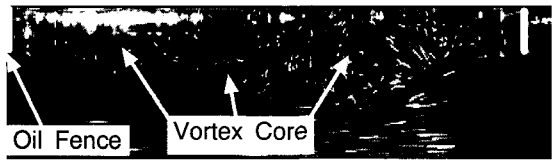

(a) without oil layer

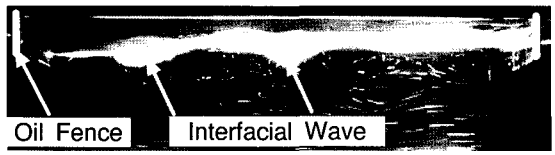

(b) with oil layer

Fig. 5 Visualization of flow (Flow is from left to right)

There may be no restriction to extend the present numerical method to the multi-layered flows by placing a vortex sheet on each interface. The flow with the free surface will be regarded as an extreme case in which the density of the upper fluid is null. The temporal evolution of the circulation at each vortex sheet can be predicted as before. Such an exact analysis considering the effect of the free surface is not performed at present. It would be, however, meaningful to examine, based on the above numerical results, whether such large-amplitude interfacial waves as observed in the experiment can be generated by the vortices detached from the tip of the fore fence. If it is assumed that the height of interfacial wave will

be of the same order of magnitude, irrespective of the existence of the free surface, what should be checked is whether the strength of the shed vortices are sufficiently large to generate such large-amplitude interfacial waves. As shown by the non-dimensionalization of the variables, the independent variables, which are related with the generation of interfacial waves, are the Froude number, the Weber number, and the density ratio. The density ratio in Fig. 5 is about 0.8 which is similar in magnitude to the case considered in the numerical analysis. As pointed out earlier, the Froude number here represents the ratio of the surface force on the interface generated by the vortices to the restoring force of gravity. To calculate the Froude and the Weber numbers, the strength of vortices and the distance between the consecutive vortices should be known.

According to the experimental results of Fage and Johansen (1927) on the characteristics of wake of a normal plate, the vortex strength (Γ_o), the distance between the consecutive vortices (L), and the convection speed of vortices (u_o) are related with the free-stream velocity (U), and the half height of the plate (D) as shown below

$$\Gamma_o = c_1 UD, \quad L = c_2 D, \quad u_o = c_3 U$$

where c_1 and c_2 are constants. Based on the experimental results of Fage and Johansen [1927], the three constants c_1, c_2, and c_3 are determined to be about 9, 10.5, and 0.77, respectively.

By definition, the characteristic length, velocity, and time become $c_2 D$, $(c_1/c_2)U$, $(c_2^2/c_1)D/U$, respectively. Then, the two numbers become

$$W = \frac{c_1^2}{c_2} \cdot \frac{\bar{\rho} DU^2}{\sigma}, \quad F = \frac{c_1}{c_2^{3/2}} \cdot \frac{U}{\sqrt{\tilde{g} D}}.$$

To calculate the values of the above variables for the case with the free surface, the constant c_1 and c_2 should be known. The value of c_2 can be determined by considering the kinematic relation of L with the shedding frequency (f) and the convection speed of the vortex. That is, the distance between two consecutive vortices can be obtained approximately as

$$L \approx u_o T = \frac{u_o}{f} = \frac{u_o H}{U \cdot St} = \frac{2c_3 D}{St} = c_2' D$$

where T is the shedding period, $St(=fH/U)$ the Strouhal number, and H the height ($2D$) of the fence.

The convection speed of vortices may not be much altered by the existence of the free surface. Thus, the value of c_3 can be used to determine the value of c_2'. Since the flow is bounded by the free surface, the flow structure will resemble the case in which a long splitter plate is placed downstream of the normal plate. According to Nakamura (1996), the Strouhal number ranges from about 0.6 to 0.23, when the length of the splitter plate is varied from $4D$ to $20D$. The corresponding values of c_2' for the two Strouhal numbers of 0.23 and 0.6 are 6.7 and 2.6, respectively.

The distance between the two troughs appearing in Fig. 5 is about $3D$. Therefore, the value of c_2' is considered to be about 3, which is between the two predicted values of 2.6 and 6.7. It is arbitrarily assumed that the strength of vorticity is 1/3 of the case without the splitter plate. Then, the value of c_1 becomes 3. The draft of the fence and free-stream velocity were $U = 0.33m/s$, $D = 0.04m$ for the results shown in Fig. 5. Then, the Weber and Froude number become 600 and 0.73, respectively. The large value of the Weber number indicates that the capillary force has no influence on the generation of such a large-scale interfacial waves. The crest-to-trough height in Fig. 5, for which the Froude number is 0.73, is about $0.15L$. In the numerical results for the Froude numbers of 0.73 shown in Fig. 4, the crest-to-trough height is about $0.3L$. As mentioned earlier, the numerical results could over-predict the interfacial wave height due to

the negligence of the viscous and free-surface effects. Based on the foregoing analysis, one can infer that the interfacial waves can be generated by the shed vortices from the tip of the fence.

4. Conclusions

1) To analyze the deformation of the oil-water interface by the vortices shedded from the tip of the fence, a numerical method is developed, replacing the vortices by a periodically distributed line vortex singularity of potential flow.
2) A linear solution for the temporal evolution of both the shape and the strength of the vortex sheet is obtained. The validity of the solution is checked by comparing the results with the numerical solution.
3) Analyses of both experimental and numerical results imply that the large-amplitude interfacial waves can be induced by the traveling vortices emanated from the tip of the fore fence.

Acknowledgement

The present investigation was carried out as a part of the project of the Environmental Fluid Mechanics Group of Advanced Fluids Engineering Research Center of Pohang University of Science and Technology. The authors gratefully acknowledge the funding support for the present investigation by Korea Science and Engineering Foundation.

References

[1] Baker, G. R., Meiron, D. I., and Orszag, A. A., 1982, "Generalized vortex methods for free-surface flow problem," *J. Fluid Mech.*, Vol. 123, 477-501.
[2] Delvigne, G. A. L., 1987, "Laboratory experiment on oil spill protection of a water intake," In: *Oil in Fresh Water: Chemistry, Biology, Counter-measure Technology*, (Eds. Vandermeulen, J. H., and Hrudey, S. E.). Pergamon Press, 446-458.
[3] Fage, A. and Johansen, F. C., 1927, "On the flow of air behind an inclined flat plate of infinite span," *Proc. Roy. Soc. A*, Vol. 116, 170-197.
[4] Lee, C. M., Kang, K. H. and Cho, N. S., 1997, "Containment capability of tandem oil fences," *Annual Report of the Advanced Fluids Engineering Research Center*, Report No. AFR-96-C, 3-48.
[5] Lee, C. M., Kang, K. H., and Cho, N. S., 1998a, "Trapping of leaked oil with tandem oil-fences with Lagrangian analysis of oil droplet motion," *J. Offshore Mech. and Arctic Eng., Trans. of the ASME*, Vol. 120, 50-55.
[6] Lee, C. M., Kang, K. H., and Han, D. G., 1998b, "On the oil-fence deflection and behavior of oil-water interface between tandem fences," *Annual Report of the Advanced Fluids Engineering Research Center*, AFR-97-CE, 3-35.
[7] Lo, J.-M., 1996, "Laboratory investigation of single floating booms and series of booms in the prevention of oil slick and jellyfish movement," *Ocean Engineering*, Vol. 23, 519-531.
[8] Longuet-Higgins, M. S., and Cokelet, E. D., 1976, "The deformation of steep surface waves on water," *Proc. Roy. Soc. Lond. A*, Vol. 350, 1-26.
[9] Milne-Thomson, L. M., 1968, *Theoretical Hydrodynamics*, Fifth ed., The University Press, Glasgow.
[10] Nakamura, Y., 1996, "Vortex shedding from bluff bodies with splitter plates," *J. Fluids and Structures*, Vol., 10, 147-158.
[11] Saffman, P. G., 1992, *Vortex Dynamics*, Cambridge Univ. Press.